Integrated platform resorting to ionic liquids comprising the extraction, purification and preservation of DNA

Teresa B.V. Dinis [a], Ana I. Valente [a], Ana P.M. Tavares [a], Fani Sousa [b,*], Mara G. Freire [a,*]

[a] CICECO – Aveiro Institute of Materials, Department of Chemistry, University of Aveiro, Aveiro, Portugal
[b] CICS-UBI – Health Sciences Research Centre, University of Beira Interior, Covilhã, Portugal

ARTICLE INFO

ABSTRACT

The large-scale production of therapeutically targeted-deoxyribonucleic acid (DNA) has passed through several challenges, postponing the tangible implementation of an effective, economic and sustainable manufacturing system. Such challenges comprise the need to develop an integrative downstream process able to extract, purify and long-term preserve DNA, whilst reducing the risk of degradation by endonucleases that would compromise their effectiveness as therapeutic products. In this work, three-phase partitioning (TPP) systems formed by the application of aqueous biphasic systems (ABS) composed of several biocompatible cholinium-based ionic liquids (ILs), are proposed for the separation of double stranded DNA (dsDNA) from the endonuclease deoxyribonuclease I (DNase I). By taking advantage of the tailor-made properties of ILs, dsDNA can be completely extracted to the IL-rich phase, whereas DNase I is precipitated at the ABS interphase. The ABS/TPP formed by IL cholinium glycolate ($[N_{111(2OH)}][Gly]$) fulfills the aim of this work, i.e. at ensuring the technical viability of IL-based ABS/TPP for the "one-pot" extraction, purification and long-term preservation of dsDNA. The results reveal the potential of this system to be applied in the bioprocessing of DNA, particularly relevant when envisioning DNA-based therapeutic products.

1. Introduction

Emerging therapeutic approaches, such as gene therapy, require the development of an efficient large-scale upstream/downstream process, in which high quantities of deoxyribonucleic acid (DNA) with high purity levels may be produced [1,2]. The effectiveness of these innovative therapies depends on the protection and correct delivery to the cells [3]. There are several examples of delivery vectors, with different characteristics, being the plasmid DNA (*p*DNA) one of the most commonly used, as it can be easily produced in a prokaryotic system [3,4]. However, from this type of production, DNA must be recovered from a complex extract containing critical impurities with similar chemical, physical and structural properties, namely, non-functional DNA isoforms, host DNA, RNA, endotoxins, endonucleases and other proteins, posing additional challenges to the downstream process [2].

The conventional methodologies to isolate and purify nucleic acids usually comprise several complex steps and often operate at high temperatures to improve the resolution, which can induce conformational stress and consequent damage to the target DNA forms [5]. Therefore, the development of strategies able to purify and preserve the biological activity and structural integrity of DNA has been addressed by the scientific community [6–11].

Aqueous biphasic systems (ABS) composed of polymers and conventional salts have been widely reported as alternative extraction and pre-purification approaches for *p*DNA [6–10]. ABS are generally composed of two water-rich phases and, if properly designed, display low-to-negligible toxicity. Several authors have successfully demonstrated the selective partition of *p*DNA from the remaining nucleic acids (RNA and genomic DNA (*g*DNA)) by controlling the parameters of ABS [6,7,10], while cell debris and contaminant proteins can be accumulated at the interphase [6,7]. These works demonstrate that ABS constitute interesting approaches for the recovery and pre-purification of *p*DNA, while being able to combine several unit operations in the downstream processing chain [6,7]. Despite the outstanding advantages of ABS, the use of high charge density salts brings some environmental concerns [9]. In addition, the narrow manipulation of the phases' polarities in salt-polymer ABS limits the recovery yields and purification factors of target DNA forms, whose denatured and sheared DNA materials are still difficult to separate from the renatured DNA forms [6–8,12]. Some of the described drawbacks may be overcome with ionic liquids (ILs),

---

* Corresponding authors.
E-mail addresses: fani.sousa@fcsaude.ubi.pt (F. Sousa), maragfreire@ua.pt (M.G. Freire).

which if properly designed, can enhance the solubility, stability and lifetime of biomolecules, such as nucleic acids [13].

One of the most attractive features of ILs falls within the scope of their designer solvents ability, in which ILs can be designed and applied to improve the performance of particular bioprocesses [14,15]. Furthermore, the discovery of new and unique biocompatible ILs [16–19] triggered the number of studies regarding the stability of nucleic acids in IL aqueous solutions [20]. Pioneering investigations revealed the successful application of biocompatible and hydrated cholinium-based ILs to maintain the structural integrity of DNA [21,22] and the biological stability of small interfering RNA [23] up to six [21] and three [23] months of storage, respectively. Further reports revealed the improvement of the DNA lifetime in aqueous solutions or neat cholinium-based ILs, while also providing information on the IL-DNA interactions [24–30].

We have recently reported a complete analysis and screening of more biocompatible structures of ILs, such as those composed of a cholinium cation, to improve the stability of DNA [31]. This work revealed that cholinium-based ILs are better preservation agents for nucleic acids when compared to the more traditional imidazolium- and phosphonium-based ILs. In the same line, and by taking advantage of the potential of cholinium-based ILs to preserve the structural stability and integrity of RNA, Quental *et al.* [32] recently proposed an integrated process based on ABS, formed by polymers and cholinium-based ILs, comprising the extraction of small RNA from bacterial lysates. However, unlike the data reported in traditional salt-polymer ABS [7], a deeper analysis of the potential use of IL-based ABS to separate impurity proteins from the nucleic acids is fundamental, in particular the endonucleases, which presence in the final product, even in trace amounts, increases the degradation rate of target nucleic acids.

The water-rich environment of IL-based ABS along with the selective precipitation of target impurities at the interphase has recently led to the proposal of these systems as three phase partitioning (ABS/TPP) systems [33]. ABS/TPP is a well-established separation technique, generally used to accumulate enzymes and proteins at the interphase, between an organic phase (usually formed with *tert*-butanol) and an aqueous phase (usually formed with ammonium sulfate), which is a valuable strategy for large-scale recovery of target compounds [34,35]. By combining the improved process biocompatibility and tunable extraction properties of IL-based ABS, IL-based ABS/TPP have been successfully applied in the recovery of proteins, such as lactoferrin, immunoglobulin G (IgG) and bovine serum albumin (BSA) [33,36–39]. ABS/TPP formed by cholinium-based ILs were also evaluated on the recovery of IgG from rabbit serum, in which albumin, the principal impurity, precipitated [39]. These promising results, where ILs successfully formed ABS/TPP with both salt and polymers, justify the evaluation of cholinium-based ILs in separating nucleic acids from undesired proteins, particularly through the precipitation of the proteins at the interphase and the extraction/recovery of the nucleic acids to the IL-rich phase.

In this work we designed IL-based ABS/TPP systems for the simultaneous extraction, pre-purification and preservation of DNA. A screening of ABS composed of several cholinium-based ILs was initially carried out to optimize the enrichment of double stranded DNA (dsDNA) into the IL-rich phase. Then, the best systems were appraised to simultaneously separate dsDNA and deoxyribonuclease I (DNase I) by the precipitation of the protein at the interphase. Finally, those systems were evaluated to preserve dsDNA at the IL-rich phase.

2. Materials and methods

2.1. Materials

dsDNA sodium salt extracted from Salmon testes (CAS no. 9007–49-2), of analytical grade, was purchased from TCI Chemicals. The 260/280 nm absorbance ratio of the DNA stock solution was found to be 1.896, indicating the absence of other proteins as impurities [40]. DNase I extracted from bovine spleen (CAS no. 9003–98-9), of analytical grade, was purchased from TCI Chemicals. The ILs studied were:

(2-hydroxyethyl)-trimethylammonium (cholinium) bromide ([N$_{111}$$_{(2OH)}$]Br), cholinium chloride ([N$_{111(2OH)}$]Cl), cholinium dihydrogen phosphate ([N$_{111(2OH)}$][DHP]), cholinium acetate ([N$_{111(2OH)}$][Ace]) and cholinium glycolate ([N$_{111(2OH)}$][Gly]). To reduce the water and volatile compounds content to negligible values ($<30 \times 10^{-6}$ in mass fraction), the ILs used in this work were dried in a vacuum line for a minimum of 48 h at (323 ± 1) K. The ILs were kept closed and stored in a desiccator up to use (maximum 48 h). The purity of each IL was checked by ^{1}H and ^{13}C nuclear magnetic resonance (NMR) spectra and found to be in accordance with the purity given by the suppliers. [N$_{111(2OH)}$] [DHP] (>98 wt% pure) and [N$_{111(2OH)}$][Ace] (>99 wt% pure) were purchased from Iolitec. [N$_{111(2OH)}$]Br (>98 wt% pure) was purchased from TCI chemicals. [N$_{111(2OH)}$]Cl (98 wt% pure) was provided by Acros Organics. [N$_{111(2OH)}$][Gly] (97 wt% pure) was synthesized by us through the neutralization of cholinium bicarbonate ([N$_{111(2OH)}$]CHO$_3$) with the respective acid, glycolic acid (1:1.10 mol ratio), at room temperature conditions according to published protocols [41]. [N$_{111(2OH)}$] CHO$_3$ (in water solution at 80 wt%) was purchased from Sigma-Aldrich. Glycolic acid (99 wt% pure) was acquired from Acros Organics. Poly (ethylene glycol) (PEG) of molecular weights of 400 and 600 g·mol^{-1} (PEG 400 and PEG 600, respectively) were acquired from Fluka and Alfa Aesar, respectively. Poly(propylene glycol) (PPG) of molecular weight of 400 g·mol^{-1} (PPG 400) was acquired from Sigma-Aldrich. Tris (hydroxymethyl)aminomethane (Tris buffer) (>99.8 wt% pure) was purchased from Pronalab. Hydrochloric acid (HCl) (in water solution at 37 wt%) was from Sigma-Aldrich. Citrate buffer (K$_3$C$_6$H$_5$O$_7$/C$_6$H$_8$O$_7$) at pH ≈ 7.0 was prepared with the mixture of potassium citrate tribasic monohydrate (K$_3$C$_6$H$_5$O$_7$·H$_2$O) (99 wt% pure from Acros Organics) and citric acid (C$_6$H$_8$O$_7$) (99.5 wt% pure from Panreac). Phosphate buffer (Na$_2$HPO$_4$/NaH$_2$PO$_4$) at pH ≈ 7.4, for chromatographic analysis, was composed of sodium hydrogen phosphate dibasic heptahydrate (Na$_2$HPO$_4$·7H$_2$O) (98–102 wt% pure from Sigma-Aldrich), sodium dihydrogen phosphate monobasic (NaH$_2$PO$_4$) (99 – 100.5 wt% pure from Panreac) and sodium chloride (NaCl) (extra pure from LabKem). The water was double distilled, passed by a reverse osmosis system and further treated with a Milli-Q plus 185 water purification apparatus (18.2 MΩ·cm at 298 K).

To perform sodium dodecyl sulphate polyacrylamide gel electrophoresis (SDS-PAGE) the following materials used: sodium dodecyl sulphate (SDS) (99 wt% pure from Acros Organics), glycerol (99 wt% pure from Acros Organics), bromophenol blue (pure from Merck), dithiothreitol (DTT) (99 wt% pure from Acros Organics), Novex™ Try-Glycine SDS Running Buffer (10 ×) (from Invitrogen™), Novex™ WedgeWell™ 16 % Tris-Glycine Gel, 15 wells (from Invitrogen™), NZYColour Protein Marker I (from Nzytech), and BlueSafe (Nzytech). For the Agarose gel Electrophoresis, Agarose (GRS Agarose LE) (molecular biology grade from Grisp Research Solutions), Xpert Green DNA Stain (20.000 ×) (from Grisp Research Solutions), 10 × Loading Buffer (from TaKaRa), NZYDNA Ladder III (from Nzytech) were used. Ethylenediamine tetra-acetic acid (EDTA) (99 wt% pure from Sigma-Aldrich), and acetic acid glacial (PA grade from Fisher Chemical), were used to make tris-acetate-EDTA (TAE) buffer 50 ×, applied in the Agarose gel Electrophoresis. The molecular structures of the investigated ILs and polymers are illustrated in Fig. 1.

2.2. Experimental procedure

2.2.1. Extraction of dsDNA

For the extraction studies, the corresponding binodal curves of the ABS must be previously determined. Most of the ternary mixture compositions selected in this work were taken from previously reported phase diagrams [42–45], except for the ternary systems composed of K$_3$C$_6$H$_5$O$_7$/C$_6$H$_8$O$_7$ + PPG 400 + H$_2$O and [N$_{111(2OH)}$]Br + PPG 400 + H$_2$O (in 100 mmol·L^{-1} of Tris·HCl (pH ≈ 7.2)). For these systems, the
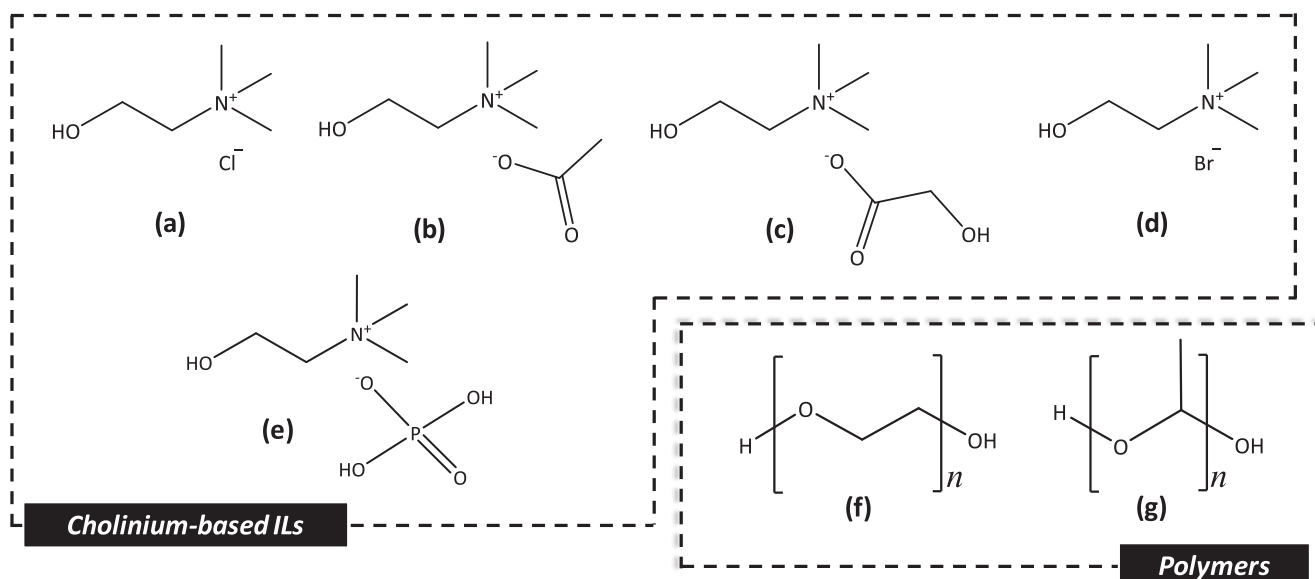
Fig. 1. Chemical structures of the investigated ABS/TPP components studied: (a) $[N_{111(2OH)}]Cl$; (b) $[N_{111(2OH)}][Ace]$; (c) $[N_{111(2OH)}][Gly]$; (d) $[N_{111(2OH)}]Br$; (e) $[N_{111(2OH)}][DHP]$; (f) PEG; (g) PPG.

binodal curves were experimentally determined in this work, as previously described [43,46]. An aqueous solution containing 1 g·L^{-1} of dsDNA in 100 mmol·L^{-1} of Tris·HCl (pH $\approx$ 7.2) was prepared. At this concentration, it is expected that dsDNA is completely solvated in aqueous medium, avoiding thus specific interactions between dsDNA macromolecules. All the partition studies were performed at variable compositions for the several polymer-based ABS investigated (detailed data available in the Supporting Information – *cf.* Table S1), with the amount of dsDNA added to each system being constant (mass fraction *ca.* 4×10^{-5}). The different binodal curves led us to work with different mixture compositions able to form liquid–liquid systems (instead of monophasic or solid–liquid mixtures). In this sense, a constant volume ratio of *ca.* 0.6 ($V_{IL\text{-rich phase}}:V_{total}$) was fixed within all the mixture compositions used in the partition studies. In IL-based ABS, the mixture points were selected to avoid discrepancies that could arise from the IL input into the system, although the common mixture composition could not be applied to the ABS constituted by $[N_{111(2OH)}]Br$ and PEG 400 since only a monophasic system was observed. On the other hand, the partition study of dsDNA was not carried out with the ABS composed of $[N_{111(2OH)}][Ace]$ and PEG 400 due to the lack of experimental points in the corresponding phase diagram [43].

Due to the high instability of nucleic acids, each ABS containing dsDNA was carefully homogenized for 60 min at 15 rpm, in a vertical rotating shaker 360° PTR-35 Grant-Bio (298 K). Then, the mixtures were centrifuged using a Megafuge 16 R centrifuge Thermo Scientific at 3500 rpm, (298 ± 1) K, during 30–60 min (depending on the system viscosity). After carefully separating both phases, the dsDNA was quantified in each phase by UV absorption spectroscopy, using a Shimadzu UV-1800, Pharma-Spec Spectrophotometer, at a wavelength of 258 nm, using a calibration curve previously established. At least three ABS for each set of conditions and three individual samples of each phase were quantified to determine the average partition coefficients and corresponding standard deviations. To remove the background of each phase-forming component in UV absorption, blank control samples were always used, while 10 mmol·L^{-1} of Tris·HCl (pH $\approx$ 7.2) was taken as blank reading and used for the dilution steps. All measurements were performed from 200 nm to 400 nm and carried out in a quartz cell with an optical path length of 10 mm.

The extraction efficiency of DNA, $EE_{dsDNA}\%$, was determined as the percentage ratio between the weight of DNA in the extractant phase and that in the total mixture, according to Equation (1):

$$EE_{dsDNA}\% = \frac{w_{Extractant}}{w_{IL} + w_{Salt}} \quad (1)$$

where $w_{Extractant}$, w_{IL} and w_{Salt} are the weights obtained for the extractant phase, IL-rich and salt-rich phases, respectively.

2.2.2. Separation/precipitation of DNase I

An aqueous solution containing 1 g·L^{-1} of DNase I in 100 mmol·L^{-1} of Tris·HCl (pH $\approx$ 7.2) was prepared. The separation studies of the endonuclease were performed with the same mixture points used for the extraction of dsDNA (*cf.* Table S1 - Supporting Information), with the amount of endonuclease in the systems kept constant (mass fraction of DNase I *ca.* 7.9×10^{-5}). Each ternary mixture containing DNase I was carefully homogenized in a vertical rotating shaker 360° PTR-35 Grant-Bio (298 K) at the same conditions used in the extraction of dsDNA. Then, mixtures were centrifuged using a Megafuge 16 R centrifuge Thermo Scientific at 3500 rpm, (298 ± 1) K, for 30–60 min (depending on the system viscosity). The top and bottom phases were separated and the interphase, containing precipitated DNase I, was resuspended in 100 mmol·L^{-1} of Tris·HCl (pH $\approx$ 7.2) and homogenized in a vertical rotating shaker 360° PTR-35 Grant-Bio (298 K).

DNase I was quantified using a Hitachi Chromaster size-exclusion high-performance liquid chromatography (SE-HPLC) equipment equipped with a binary pump, column oven operating at (313 ± 1) K, temperature controlled auto-sampler operating at (283 ± 1) K, diode-array detector and a column Shodex Protein KW-802.5 (8 mm × 300 mm). Standard aqueous solutions of DNase I at known concentration, as well as IL and polymer aqueous solutions spiked with DNase I at known concentrations, were used to validate the flow and composition of the mobile phase, whose conditions have been previously established [33]. The mobile phase consisted of Na$_2$HPO$_4$/NaH$_2$PO$_4$ buffer (at 50 mmol·L^{-1}, pH $\approx$ 7.4, with NaCl at 0.3 M), with an isocratic run at a flow rate of 0.5 mL·min^{-1}. The mobile phase was filtered before use with 0.45 μm regenerated cellulose membrane filters from Whatman. Individual standard aqueous solutions of DNase I were prepared (0.25 g·L^{-1}) and periodically injected in order to compare the peak areas of the endonuclease obtained in the aqueous standard solutions and in the samples. Before injection in SE-HPLC, all samples were diluted in 100 mmol·L^{-1} of Tris·HCl (pH $\approx$ 7.2). The wavelength was set at 280 nm. DNase I chromatographic peaks were analyzed to determine the weight percentage of

the endonuclease at the interphase and in the top and bottom phases. At least three replicates were carried out for the interphase and the top and bottom phases to ascertain the standard deviations. Blank controls of the systems were always used to check for possible interferences of the phase-forming components in the peak retention time of DNase I.

2.2.3. Simultaneous separation of dsDNA from DNase I

The same mixture points used for the individual extraction and precipitation studies of dsDNA and DNase I were evaluated for simultaneously separate both biomolecules. Each ternary mixture containing DNase I was carefully homogenized in a vertical rotating shaker 360° PTR-35 Grant-Bio (298 K) at the same conditions for 58 min. Then, the dsDNA was added to the system and homogenized for 2 min (total time 60 min). Both biomolecules were in the same mass fraction as used previously, ca. 4×10^{-5} for dsDNA and ca. 7.9×10^{-5} for DNase I. The system containing both dsDNA and DNase I was centrifuged using a Megafuge 16 R centrifuge Thermo Scientific at 3500 rpm, at (298 ± 1) K, for 30–60 min (depending on the system viscosity). The top and bottom phases were separated. The interphase containing precipitated DNase I was resuspended in 100 mmol·L^{-1} Tris·HCl (pH $\approx$ 7.2) and homogenized in a vertical rotating shaker 360° PTR-35 Grant-Bio (298 K). Both biomolecules were quantified in the recovered interphase, and in top and bottom phases through SE-HPLC. Standard aqueous solutions of pure DNase I, pure dsDNA and a mixture of DNase I and dsDNA at known concentration were periodically injected in order to compare the peak areas obtained in the aqueous standard solutions and in the samples. Before injection in SE-HPLC, all samples were diluted in 100 mmol·L^{-1} of Tris·HCl (pH $\approx$ 7.2). At least three replicates of each sample were carried out. Blank controls of the systems were always used to check for possible interferences of the ABS/TPP phase-forming components.

2.2.4. SDS-PAGE

SDS-PAGE was used to assess the presence of DNase I in each ABS phase. After the separation of the phases, iced ethanol was added (dilution factor of 4) to the samples and stored at 253 K for 2 h. To recover the precipitated dsDNA and DNase I, the samples were centrifuged in a Megafuge 16 R centrifuge Thermo Scientific at 10000 rpm, (277 ± 1) K for 30 min. The supernatant was recovered and discarded, and the precipitate was resuspended in 60 µL of Tris HCl 100 mmol·L^{-1} (pH $\approx$ 7.2). The samples were diluted at a 1:1 (v/v) ratio in a sample buffer (composed by 2.5 mL of 0.5 M Tris HCl pH 6.8, 4.0 mL of 10 % (w/v) SDS solution, 2.0 mg of bromophenol blue, 2.0 mL of glycerol and 310 mg of DTT) and heated for 5 min at 368 K. 20 µL of all samples were loaded and run at 100 V on a polyacrylamide gel. NZYColour Protein Marker I was used as molecular weight standards while commercial DNase I was used as DNase I standard. To stain the proteins, the gels were impregnated with BlueSafe and stirred in an Heidolph^{TM} rotamax 120 orbital shaker at 50 rpm for 40 min at room temperature.

2.2.5. Agarose gel electrophoresis

Agarose gel electrophoresis was performed to assess the presence of dsDNA in each ABS phase. As for SDS-PAGE, the phases were treated with iced ethanol and the biomolecules recovered through centrifugation after their precipitation. A gel with 1 % (w/v) of agarose was prepared by the dissolution of agarose in 100 mL of heated TAE buffer ($\approx$373 K). After the dissolution, the solution was cooled down until $\approx$328 K and at that point, 1.4 µL of Xpert Green DNA Stain was added. Lastly, the solution was poured into a tray, where a well-former template is placed across the end of the tray to form wells when the gel solution solidifies. The samples were diluted at 9:1 (v/v) ratio in a loading buffer (10 $\times$ Loading Buffer from TaKaRa). 25 µL of all samples were loaded and run at 100 V on the agarose gel. NZYDNA Ladder III was used as molecular weight standards while commercial dsDNA was used as dsDNA standard. The bands were revealed through exposure to UV radiation in a VWR GenoSmart2.

2.2.6. Circular dichroism spectroscopy

dsDNA secondary structure in the bottom phases was evaluated by circular dichroism (CD) spectroscopy using a Jasco J-1500CD spectrometer. A solution of DNA standard 0.04 g·L^{-1} was analyzed as a control. CD spectra were recorded at room temperature in the far UV region, from 220 to 350 nm, using quartz CD cuvettes (0.1 cm) at a scan rate of 50 nm.min^{-1} and sensitivity of 100 mdeg. The response time and the bandwidth were 8 s and 1 nm, respectively.

2.2.7. Quantification of water in the coexisting phases

The water content of the coexisting phases was determined for the same mixture points used in the partition studies. The water amount in each phase was gravimetrically determined ($\pm 10^{-4}$ g) by evaporation, using an air oven at.

(353 ± 1) K, until a constant weight of the non-volatile mixture (Polymer + IL/Salt/Polymer) was achieved. This process was carried out in triplicate to ascertain the associated standard deviations.

2.2.8. pH and conductivity measurements

After phase separation, the pH values (± 0.02) and conductivities ($\pm 10^{-5}$ S·cm^{-1}) of each phase were determined at (298 ± 1) K using a SevenMulti (METTLER TOLEDO Instruments). The IL/salt-rich and polymer-rich phases were identified by conductivity values.

3. Results and discussion

3.1. dsDNA extraction

In this work, commercial dsDNA with linear conformation was used for the extraction studies in IL-based ABS. The use of the same ILs studied in our previous work regarding the DNA stability [31] allows to establish an insightful evaluation on the dsDNA extraction mechanisms. Due to their promising results to stabilize the structural conformation of dsDNA, the following cholinium-based ILs, namely [N$_{111(2OH)}$]Br, [N$_{111(2OH)}$]Cl, [N$_{111(2OH)}$][DHP], [N$_{111(2OH)}$][Ace] and [N$_{111(2OH)}$][Gly], were used to create ABS. Moreover, two polymers with different hydrophobicity, namely PPG 400 and PEG 400, were used to form ABS with cholinium-based ILs to gather a deeper understanding on the mechanisms responsible for dsDNA partitioning among the two phases. For comparison purposes, the partition behaviour of dsDNA was also pursued by traditional ABS. For polymer–polymer ABS, PEG 400 and PPG 400 were combined in aqueous media to induce liquid–liquid equilibrium. For salt-polymer ABS, the ternary mixtures K$_3$C$_6$H$_5$O$_7$/C$_6$H$_8$O$_7$ + PEG 400 (or PPG 400) + H$_2$O were selected, since K$_3$C$_6$H$_5$O$_7$/C$_6$H$_8$O$_7$ is a biological and biodegradable buffer. Before the extraction studies of dsDNA with ABS, its structural stability was evaluated using CD in aqueous solutions of the polymers and citrate buffer in 10 mmol·L^{-1} Tris·HCl (pH $\approx$ 7.2), accordingly to our previous work [31]. CD analysis also allowed to *a priori* verify the existence of structural changes in dsDNA that could compromise the analysis and quantification of the macromolecule after the extraction step. No significant changes on dsDNA conformation were observed, with exception of PPG 400 that presents a negative effect on dsDNA stability at higher concentrations (*cf.* Figure S1 - Supporting Information), as a result of the stronger acidic environment provided by the presence of the polymer in solution. In this sense, and with the exception of the ABS composed of the citrate buffer, ABS were prepared at a higher concentration of buffer, 100 mmol·L^{-1} of Tris·HCl (pH $\approx$ 7.2), in order to avoid pH fluctuations that could affect the dsDNA stability and structural integrity during extraction procedures, allowing to maintain the pH of the coexisting phases between 6 and 8 (*cf.* Table S1 - Supporting Information).

For the extraction studies, most of ternary mixture compositions selected in this work were taken considering previously reported phase diagrams [42–45], with the exception of the ternary systems composed of K$_3$C$_6$H$_5$O$_7$/C$_6$H$_8$O$_7$ + PPG 400 + H$_2$O and [N$_{111(2OH)}$]Br + PPG 400 + H$_2$O (in 100 mmol·L^{-1} of Tris·HCl (pH $\approx$ 7.2)). For these systems, the

binodal curves are represented in the Supporting Information (Figure S2), with the experimental weight fraction data of each system given as well in the Supporting Information (Tables S2 to S4).

Fig. 2 depicts the extraction efficiencies of dsDNA and water distribution between the coexisting phases, ΔH_2O, in the various ABS investigated: PEG 400 + PPG 400; $K_3C_6H_5O_7/C_6H_8O_7$ + PEG 400; $K_3C_6H_5O_7/C_6H_8O_7$ + PPG 400; $K_3C_6H_5O_7/C_6H_8O_7$ + PEG 600; $[N_{111(2OH)}]Cl$ + PEG 400; $[N_{111(2OH)}]Cl$ + PPG 400; $[N_{111(2OH)}]Cl$ + PEG 600; $[N_{111(2OH)}][Gly]$ + PEG 400; $[N_{111(2OH)}][Gly]$ + PPG 400; $[N_{111(2OH)}][DHP]$ + PEG 400; $[N_{111(2OH)}][DHP]$ + PPG 400; $[N_{111(2OH)}][Ace]$ + PPG 400; $[N_{111(2OH)}]Br$ + PPG 400. Further details are given in the Supporting Information (Table S5). The coexisting phases were identified by conductivity and water content measurements (experimental data given in the Supporting Information – cf. Table S1). In general, the bottom phase corresponds to IL- or salt-rich phase while the top phase corresponds to the polymer-rich phase. However, an inversion in the type of the phases is observed for the ABS composed of $[N_{111(2OH)}]Cl$ and PEG 400, where the top phase corresponds to the IL-rich phase and the bottom phase to the polymer-rich phase. This switch of phases was also tested by the increase of the molecular weight of PEG, in this case using PEG 600, where the same behaviour was observed. Regarding the polymer–polymer ABS composed of PEG 400 and PPG 400, PEG 400-rich phase was assumed as the bottom phase due to its higher water content, since PEG 400 is less hydrophobic than PPG 400. Moreover, and according to the literature [47,48], PEG 400 is denser than PPG 400 due to its shorter aliphatic chains.

For all ABS containing PPG 400, dsDNA is completely extracted to the bottom phase, as well as for the systems containing the cholinium-based ILs and PEG 400 (Fig. 2 – A). The higher water content differences between the coexisting phases clearly show a lower water distribution profile (Fig. 2 – B), supporting the stronger affinity of dsDNA to the water-rich phase (bottom phase). An exception is observed for the ABS composed of PEG 400 and PPG 400, where dsDNA partially partitions to the bottom phase (PEG 400-rich) and the remaining nucleic acid is precipitated (cf. Figure S3 - Supporting Information). dsDNA precipitation in the presence of polymers, in particular PEG, has been already reported [49]. This phenomenon was mimicked in this work through the preparation of dsDNA by aqueous solutions of high concentration of Tris·HCl buffer (pH $\approx$ 7.2) (at 1000 mmol·L^{-1}) and 30 wt% of PPG 400

and PEG 400 (cf. Figure S3 - Supporting Information). Upon the addition of dsDNA into the solutions, the instantaneous precipitation of the nucleic acid occurs, thus supporting the partition behaviour observed in the ABS composed of PEG 400 and PPG 400. On the other hand, in the ABS composed of $K_3C_6H_5O_7/C_6H_8O_7$ + PEG 400, dsDNA is completely extracted to the polymer-rich phase. The preferential partition of nucleic acids to the polymer-rich phase was already reported by Prazeres and co-workers [6], where pDNA partitions to the PEG-rich phase for polymers with lower molecular weight.

In order to better understand the impact of the polymer hydrophobicity on the extraction of dsDNA, the increase of the molecular weight of PEG was investigated. In particular, with ABS containing citrate buffer and PEG 600, the same partition behaviour of dsDNA was observed (Fig. 2 – A). These results demonstrate that size exclusion does not present a major role on the DNA partition behaviour in PEG-ABS, as proposed by some authors [6,9,10]. On the other hand, in all ABS composed of ILs, DNA is completely extracted to the IL-rich phase, regardless the hydrophobicity and/or molecular weight of the polymer. Further experimental data demonstrate a high and similar water distribution between the coexisting phases in all PEG-ABS (Fig. 2 – B), without a defined trend to support the change of dsDNA partition from the top to the bottom phases.

Although dsDNA is a negatively charged macromolecule due to the presence of a double chain of negative phosphate groups surrounding the external structure of the macromolecule, Fig. 2-A demonstrate different dsDNA migration patterns between the coexisting phases. Regardless the phase-forming components, the results suggest that specific and favourable interactions might exist between dsDNA and the extractant phase. Nevertheless, an adequate determination of the respective tie-lines towards the analytical quantification of the phase-forming components in each phase is unavoidable to further understand the extraction mechanism of dsDNA and to further design IL-based ABS more prone to specific DNA forms.

3.2. DNase I precipitation

The permanent damage of DNA often results in a complete inhibition of downstream applications [50] that are essential to guarantee the therapeutic effectiveness of DNA products. The long-term storage and
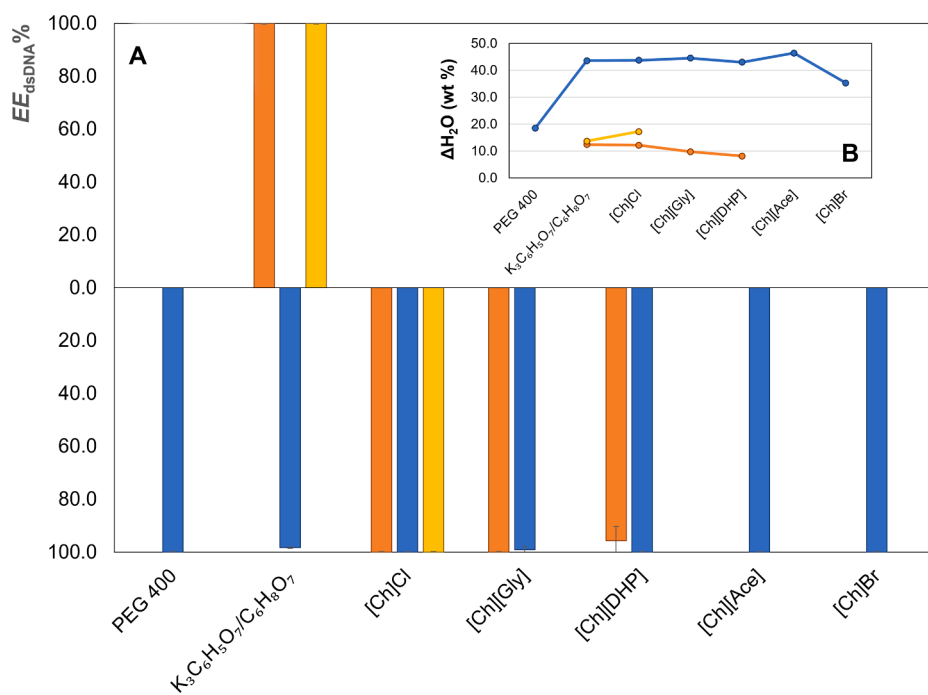

Fig. 2. (A) Extraction efficiency of dsDNA, $EE_{dsDNA}\%$, and (B) water variation, ΔH_2O, in ABS composed of IL or salt or polymer (1) + Polymer (2) + 100 mmol·L^{-1} Tris·HCl (pH $\approx$ 7.2). ΔH_2O represents the difference in weight percentage between the water content in the IL/salt/polymer (1)-rich and polymer-rich phases. Polymer (2): ($\bullet$) PEG 400; ($\bullet$) PEG 600; ($\bullet$) PPG 400. ABS order, from left to right: PEG 400 + PPG 400 + H_2O; $K_3C_6H_5O_7/C_6H_8O_7$ + PEG 400 + H_2O; $K_3C_6H_5O_7/C_6H_8O_7$ + PPG 400 + H_2O; $K_3C_6H_5O_7/C_6H_8O_7$ + PEG 600 + H_2O; $[N_{111(2OH)}]Cl$ + PEG 400 + H_2O; $[N_{111(2OH)}]Cl$ + PPG 400 + H_2O; $[N_{111(2OH)}]Cl$ + PEG 600 + H_2O; $[N_{111(2OH)}][Gly]$ + PEG 400 + H_2O; $[N_{111(2OH)}][Gly]$ + PPG 400 + H_2O; $[N_{111(2OH)}][DHP]$ + PEG 400 + H_2O; $[N_{111(2OH)}][DHP]$ + PPG 400 + H_2O; $[N_{111(2OH)}][Ace]$ + PPG 400 + H_2O; $[N_{111(2OH)}]Br$ + PPG 400 + H_2O. In all the systems the water used corresponds to an aqueous solution containing 100 mmol·L^{-1} of Tris·HCl to guarantee the pH $\approx$ 7.2.

preservation of DNA is a mandatory step to develop delivery strategies for genetic material with therapeutic purposes, such as gene therapy or DNA vaccination, avoiding their susceptibility to chemical or enzymatic degradation [51,52]. DNA is particularly vulnerable to DNase I, an endonuclease that non-specifically degrades single and double stranded DNA, preferentially by the cleavage of alternating pyrimidine/purine sequences, thus posing a great challenge for the long-term storage of DNA [53].

The same ABS used in the extraction of dsDNA were employed to investigate the removal by precipitation of DNase I. Upon the addition of DNase I, a light and thin layer was observed at the interphase of the ABS, resulting from the partial or complete accumulation of the endonuclease at the interphase (*cf.* Figure S4 in the Supporting Information). Even though IL-based ABS/TPP have been reported for the recovery of valuable proteins [36–38], the accumulation of impurities at the interphase can be a different and useful approach for the pre-purification of target products from real and complex matrices. The suitability of the investigated ABS/TPP to induce the precipitation of DNase I is summarized in Table 1.

The data presented in Table 1 evidence the formation of ABS/TPP for all systems composed of PEG, whilst for systems containing PPG 400 the formation of the protein layer at the interphase is not observed. Furthermore, the formation of the precipitate at the interphase is favoured by the increase of the PEG molecular weight. Overall, the qualitative trend shown in Table 1 is useful to identify the most promising systems able to remove DNase I by its precipitation at the interphase, whereas dsDNA should be recovered with high stability in one of the ABS phases.

The recovery of the interphase and both liquid phases was additionally carried out and DNase I was quantified by SE-HPLC, whose results are shown in Table 2. An example of the obtained chromatograms with the peak profile of DNase I, recovered from the interphase and in both liquid phases of IL-based ABS/TPP, is provided in the Supporting Information – *cf.* Figure S5.

According to the mass balance calculations for endonuclease, it can

Table 1
Main characteristics of the systems prepared to evaluate the partition of DNase I.

System	System composition		Main characteristics	
	100 w_1	100 w_2	Two liquid phases	DNase I layer at the interphase
Polymer (1)-Polymer (1)				
PEG 400-PPG 400	33.0	40.0	✓	✗
Salt (1)-Polymer (2)				
Citrate buffer-PEG 400	30.0	35.0	✓	✓
Citrate buffer-PEG 600	30.0	35.0	✓	✓
Citrate buffer-PPG 400	11.3	37.2	✓	✗
IL (1)-Polymer (2)				
[N$_{111(2OH)}$]Cl-PEG 400	41.3	45.0	✓	✓
[N$_{111(2OH)}$]Cl-PEG 600	41.3	45.0	✓	✓
[N$_{111(2OH)}$]Cl-PPG 400	11.3	37.2	✓	✗
[N$_{111(2OH)}$][Gly]-PEG 400	41.3	45.0	✓	✓
[N$_{111(2OH)}$][Gly]-PPG 400	11.3	37.2	✓	✗
[N$_{111(2OH)}$][DHP]-PEG 400	41.3	45.0	✓	✓
[N$_{111(2OH)}$][DHP]-PPG 400	11.3	37.2	✓	✗
[N$_{111(2OH)}$][Ace]-PPG 400	11.3	37.2	✓	✗
[N$_{111(2OH)}$]Br-PPG400	17.0	41.0	✓	✗

Table 2
Distribution profiles of DNase I among the "three phases" formed by the ABS/TPP composed of Salt-Polymer and IL-Polymer.

System	Distribution of DNase I among the phases			DNase redissolution
	100 w_{Top}	100 $w_{interphase}$	100 w_{Bottom}	
Salt-Polymer				
Citrate buffer-PEG 400	0.00	100.0 ± 0.2	0	✗
Citrate buffer-PEG 600	0.00	100.0 ± 0.2	0	✗
IL-Polymer				
[N$_{111(2OH)}$]Cl-PEG 400	85.53 ± 0.35	14.47 ± 0.35	0	✓
[N$_{111(2OH)}$]Cl-PEG 600	25.95 ± 0.61	74.05 ± 0.61	0	✓
[N$_{111(2OH)}$][Gly]-PEG 400	0	100.0 ± 0.2	0	✗
[N$_{111(2OH)}$][DHP]-PEG 400	0	100.0 ± 0.2	0	✗

be concluded that the precipitate layers described in Table 2 correspond to the DNase I accumulated at the interphase of each ABS/TPP. It should be also mentioned that the amount of DNase I added to the systems was constant in all experiments (mass fraction of DNase I *ca.* 7.9×10^{-5}) so that the differences on the amount of DNase I precipitated at the interphase could be only influenced by the type and composition of the phase-forming components in the ABS/TPP.

According to the data shown in Table 2, the DNase I accumulation at the interphase was only observed in the PEG-containing systems; the higher differences in the water distribution between the two liquid phases observed for PPG when compared to PEG (Fig. 2 - B) can probably explain the higher affinity of DNase I to the phases richer in water in PPG-containing systems. It is also seen that the increase of the PEG molecular weight favours the accumulation of DNase I at the interphase, which also seems to follow the higher water distribution for PEG 600-containing systems when compared to PEG 400-based ABS (Fig. 2 - B). Another important aspect described in Table 2 is the endonuclease redissolution process. With the exception of the [N$_{111(2OH)}$]Cl-based ABS/TPP, DNase I cannot be completely redissolved. The same behaviour was observed by Alvarez-Guerra and Irabien [38] for the proteins lactoferrin and BSA, where the authors associated the proteins redissolution disability to conformational changes in their structures. Because of this situation, the DNase I recovered from the interphase could not be quantified, being alternatively determined by mass balance through the determination of the protein in each ABS phase.

Contrarily to the observed in salt-polymer ABS/TPP, where complete interfacial precipitation of DNase I is always observed, it is possible to optimize the recovery of DNase I at the interphase for ABS/TPP composed of ILs (Table 2). At a fixed mixture composition and PEG 400 (Table 1), the interfacial accumulation ability of DNase I is dependent on the IL (anion) structure and follows the trend: [N$_{111(2OH)}$]Cl < [N$_{111(2OH)}$][Gly] ≈ [N$_{111(2OH)}$][DHP]. Complete accumulation of DNase I at the interphase was observed for systems comprising [N$_{111(2OH)}$][Gly] and [N$_{111(2OH)}$][DHP], in which no DNase I were observed in the ABS coexisting phases. Apart from [N$_{111(2OH)}$][DHP] that provides more acidic conditions to the solutions, the denaturation of the DNase I was also observed in systems comprising [N$_{111(2OH)}$][Gly], in which the complete endonuclease redissolution was not possible (Table 2). On the other hand, for the system composed of [N$_{111(2OH)}$]Cl, the complete redissolution of DNase I recovered from the interphase was observed during the experiments, meaning that the preservation and/or renaturation of DNase I is possible in [N$_{111(2OH)}$]Cl-based ABS/TPP. Based on the results gathered, it can be concluded that the IL structure and the water distribution among the coexisting phases play the major roles for the optimization of the DNase I recovery at the interphase of ABS/TPP, whilst the conformational change of the endonuclease can be controlled

by a proper choice of the IL anion. Therefore, other classes of ILs (with different cation and anion combinations) should be sought to perform additional studies on the structure and conformational changes that DNase I might suffer. Overall, $[N_{111(2OH)}][Gly]$ clearly fulfills the aim of this work in order to ensure the technical viability of the extraction, purification and preservation of dsDNA from the contaminant DNase I.

3.3. Integrated process for the simultaneous extraction, (pre)purification and preservation of pDNA

Even though linear dsDNA was here employed for the partition studies using IL-based ABS, due to the promising results found in our work, we suggest the development of an integrated process for "one-pot" extraction, pre-purification and preservation strategy of nucleic acids, namely *p*DNA products, using IL-based ABS/TPP. Considering the previous data, the system composed of $[N_{111(2OH)}][Gly]$ and PEG 400 fulfills the complete extraction of the target nucleic acid to the IL-rich phase, the complete interfacial precipitation of DNase I, and can guarantee the long-term storage of nucleic acids in the $[N_{111(2OH)}][Gly]$-rich phase [25]. Moreover, it has been shown that IL-based media allow to preserve nucleic acids stability and integrity at room temperature [21,25,32], thus reducing the energy consumption associated to the conventional refrigeration protocols for DNA-containing samples (277 K and 193 K for short- and long-term storage, respectively) [54].

As a proof of concept, a mixture of dsDNA and DNase I was added to the system composed of $[N_{111(2OH)}][Gly]$ and PEG 400 in order to verify if the partitioning behaviour of the individual biomolecules is maintained and if the dsDNA secondary structure is preserved after the extraction process. Fig. 3-A and 4-B present the results of SDS-PAGE and agarose gel electrophoresis, respectively. As depicted in Fig. 3-A, when both dsDNA and DNase I are present in the ABS/TPP, DNase I precipitates at the interphase, according to the presence of its characteristic band at $\approx$ 31 kDa. The absence of bands in the top and bottom phases indicates the complete precipitation of DNase I. Relatively to the partition of dsDNA (Fig. 3-B), a band with high intensity is present in the lane corresponding to the bottom phase, and no dsDNA is detected in the top

phase, evidencing that the partition behaviour of dsDNA is kept the same in. However, a low intensity band also appears at the interphase, meaning that a low amount of DNA can be lost and that further optimizations should be performed when considering this process for large-scale applications.

The structure of dsDNA, after the partition, was evaluated through CD spectroscopy, whose results are shown in Fig. 4. The resultant spectra present a positive band around 280 nm and a negative around 245 nm for both samples: a 0.04 g.L^{-1} dsDNA control solution in 100 mmol·L^{-1} Tris· HCl pH 7.2 and the bottom phase of an ABS. The results are in accordance with the literature [31,55], indicating that dsDNA maintained its structural stability after the extraction to the IL-rich phase.

These results demonstrate that, if properly designed, IL-based ABS/ TPP allow the simultaneous extraction of dsDNA to the IL-rich phase and the endonuclease DNase I precipitation at the ABS interphase.
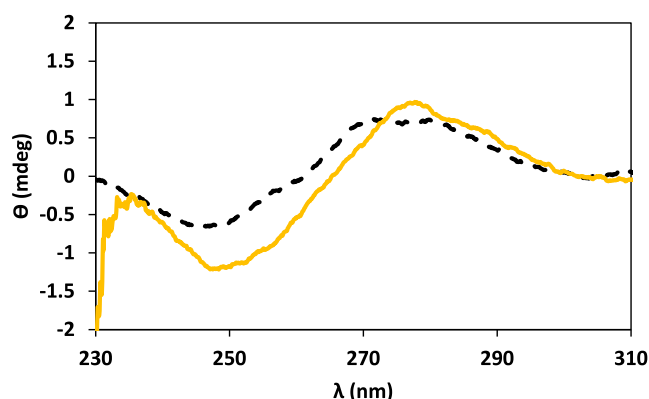

Fig. 4. CD spectra regarding the structural stability of dsDNA, after its partition into the IL-based ABS/TPP composed of 41.3 wt% $[N_{111(2OH)}][Gly]$ + 45 wt% PEG 400, (yellow line) and in Tris HCl 100 mmol·L^{-1} pH 7.2 (black dashed) in a concentration of 0.04 g.L^{-1}. (For interpretation of the references to colour in this figure legend, the reader is referred to the web version of this article.)
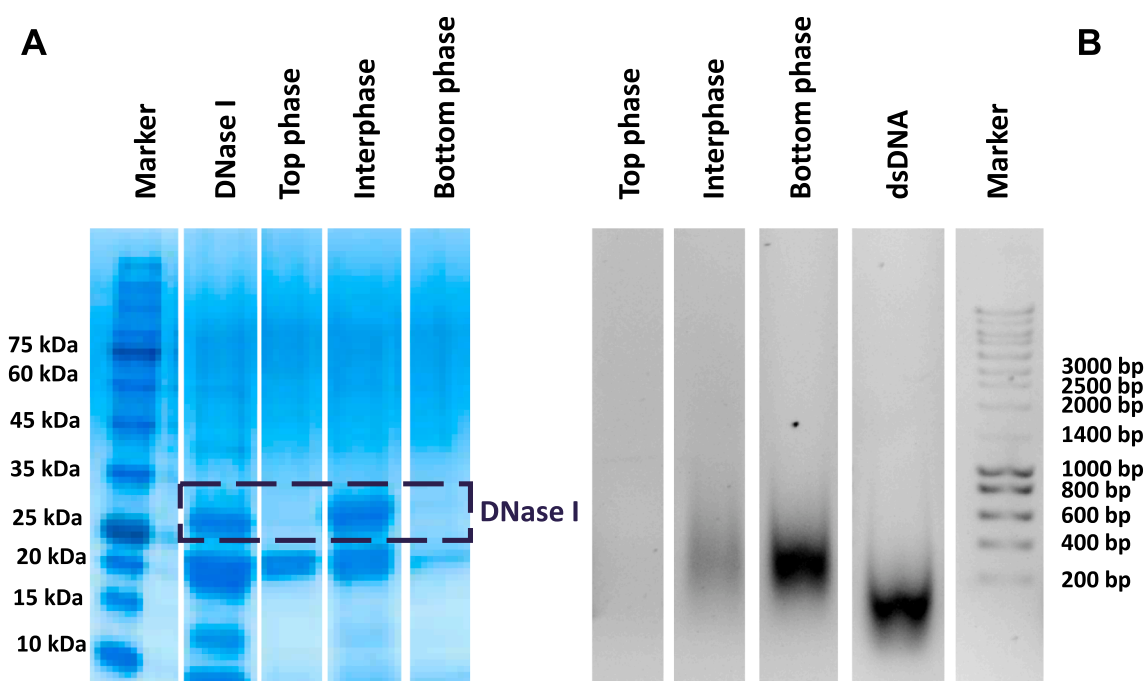

Fig. 3. (A) SDS-PAGE stained with BlueSafe for the detection of DNase I in the different phases of an ABS/TPP composed of 41.3 wt% $[N_{111(2OH)}][Gly]$ + 45 wt% PEG 400, with both macromolecules. (B) Agarose gel electrophoresis for the qualitative detection of DNase I in the different phases of an ABS/TPP composed of 41.3 wt% $[N_{111(2OH)}][Gly]$ + 45 wt% PEG 400, with both macromolecules.

Furthermore, in our work, the compounds used are low cost, while being water-rich and thus requiring low amounts of the remaining phase-forming components when compared to traditional liquid–liquid systems. Compared with a commercial Kit, such as QIAGEN Plasmid Midi Kit for 25 extractions that costs around $379 [56], our method allows the same number of extractions and amount of DNA purified by $31.32. This value was calculated taking into account the price of the reagents used for the synthesis of $[N_{111(2OH)}][Gly]$ [57,58] and PEG 400 [59] necessary to perform the described number of extractions. Still, the price of these compounds correspond to their acquisition at the lab scale; if their production is scaled-up to be implemented at a larger scale the cost of the developed IL-based ABS/TPP process will decrease even more.

4. Conclusions

It was here shown that properly designed IL-based ABS/TPP allow the simultaneous extraction of dsDNA to the IL-rich phase and the endonuclease DNase I precipitation at the ABS interphase, in which the best results were obtained with the systems containing the ILs $[N_{111(2OH)}][Gly]$ and $[N_{111(2OH)}][DHP]$. To this end, a screening of ABS composed of several cholinium-based ILs was carried out to optimize the enrichment of dsDNA into the IL-rich phase. Then, the best systems were appraised to simultaneously separate dsDNA and DNase I by the precipitation of the protein at the interphase. Finally, those systems were evaluated to preserve DNA at the IL-rich phase. Due to its biocompatible features, $[N_{111(2OH)}][Gly]$ fulfills the aim of this work at ensuring the technical viability of IL-based ABS/TPP for the "one-pot" extraction, purification and preservation of dsDNA, as experimentally demonstrated, whose results are expected to be transposed to other DNA types as advanced therapy products.

CRediT authorship contribution statement

Teresa B.V. Dinis: Data curation, Formal analysis, Investigation, Methodology, Writing – original draft. **Ana I. Valente:** Data curation, Formal analysis, Investigation, Writing – original draft, Writing – review & editing. **Ana P.M. Tavares:** Funding acquisition, Methodology, Validation, Writing – review & editing. **Fani Sousa:** Conceptualization, Funding acquisition, Methodology, Project administration, Resources, Writing – review & editing, Validation. **Mara G. Freire:** Conceptualization, Funding acquisition, Methodology, Project administration, Resources, Writing – review & editing, Validation, Supervision.

Declaration of Competing Interest

The authors declare that they have no known competing financial interests or personal relationships that could have appeared to influence the work reported in this paper.

Data availability

Data will be made available on request.

Acknowledgments

Appendix A. Supplementary data

Supplementary data to this article can be found online at https://doi.org/10.1016/j.seppur.2023.123646.

References

[1] J. Ohlson, Plasmid manufacture is the bottleneck of the genetic medicine revolution, Drug Discov. Today 25 (2020) 1891–1893, https://doi.org/10.1016/j.drudis.2020.09.040.

[2] X. Wang, L. Zhao, X. Wu, H. Luo, D. Wu, M. Zhang, J. Zhang, M. Pakvasa, W. Wagstaff, F. He, Y. Mao, Y. Zhang, C. Niu, M. Wu, X. Zhao, H. Wang, L. Huang, D. Shi, Q. Liu, N. Ni, K. Fu, K. Hynes, J. Strelzow, M. El Dafrawy, T.-C. He, H. Qi, Z. Zeng, Development of a simplified and inexpensive RNA depletion method for plasmid DNA purification using size selection magnetic beads (SSMBs), Genes Dis. 8 (2021) 298–306, https://doi.org/10.1016/j.gendis.2020.04.013.

[3] J.J. Suschak, J.A. Williams, C.S. Schmaljohn, Advancements in DNA vaccine vectors, non-mechanical delivery methods, and molecular adjuvants to increase immunogenicity, Hum. Vaccin. Immunother. 13 (2017) 2837–2848, https://doi.org/10.1080/21645515.2017.1330236.

[4] P.N. Matkar, H. Leong-Poi, K.K. Singh, Cardiac gene therapy: are we there yet? Gene Ther. 23 (2016) 635–648, https://doi.org/10.1038/gt.2016.43.

[5] É. Mota, Á. Sousa, U. Černigoj, J.A. Queiroz, C.T. Tomaz, F. Sousa, Rapid quantification of supercoiled plasmid deoxyribonucleic acid using a monolithic ion exchanger, J. Chromatogr. A 1291 (2013) 114–121, https://doi.org/10.1016/j.chroma.2013.03.070.

[6] S.C. Ribeiro, G.A. Monteiro, J.M.S. Cabral, D.M.F. Prazeres, Isolation of plasmid DNA from cell lysates by aqueous two-phase systems, Biotechnol. Bioeng. 78 (2002) 376–384, https://doi.org/10.1002/bit.10227.

[7] A. Frerix, M. Müller, M.R. Kula, J. Hubbuch, Scalable recovery of plasmid DNA based on aqueous two-phase separation, Biotechnol. Appl. Biochem. 42 (2005) 57–66, https://doi.org/10.1042/ba20040107.

[8] A. Frerix, M. Schönewald, P. Geilenkirchen, M. Müller, M.R. Kula, J. Hubbuch, Exploitation of the coil-globule plasmid DNA transition induced by small changes in temperature, pH salt, and poly(ethylene glycol) compositions for directed partitioning in aqueous two-phase systems, Langmuir 22 (2006) 4282–4290, https://doi.org/10.1021/la052745u.

[9] G.A. Gomes, A.M. Azevedo, M.R. Aires-Barros, D.M.F. Prazeres, Purification of plasmid DNA with aqueous two phase systems of PEG 600 and sodium citrate/ammonium sulfate, Sep. Purif. Technol. 65 (2009) 22–30, https://doi.org/10.1016/j.seppur.2008.01.026.

[10] F. Luechau, T.C. Ling, A. Lyddiatt, Selective partition of plasmid DNA and RNA in aqueous two-phase systems by the addition of neutral salt, Sep. Purif. Technol. 68 (2009) 114–118, https://doi.org/10.1016/j.seppur.2009.04.016.

[11] H.M. Zhang, Y.Z. Wang, Y.G. Zhou, K.J. Xu, N. Li, Q. Wen, Q. Yang, Aqueous biphasic systems containing PEG-based deep eutectic solvents for high-performance partitioning of RNA, Talanta 170 (2017) 266–274, https://doi.org/10.1016/j.talanta.2017.04.018.

[12] B. Nazer, M.R. Dehghani, B. Goliaei, Plasmid DNA affinity partitioning using polyethylene glycol – sodium sulfate aqueous two-phase systems, J. Chromatogr. B 1044–1045 (2017) 112–119, https://doi.org/10.1016/j.jchromb.2017.01.002.

[13] M. Sivapragasam, M. Moniruzzaman, M. Goto, Recent advances in exploiting ionic liquids for biomolecules: Solubility, stability and applications, Biotechnol. J. 11 (2016) 1000–1013, https://doi.org/10.1002/biot.201500603.

[14] A. Dimitrijević, A.P.M. Tavares, A. Jocić, S. Marić, T. Trtić-Petrović, S. Gadžurić, M.G. Freire, Aqueous biphasic systems comprising copolymers and cholinium-based salts or ionic liquids: Insights on the mechanisms responsible for their creation, Sep. Purif. Technol. 248 (2020) 117050, https://doi.org/10.1016/j.seppur.2020.117050.

[15] N. Nasirpour, M. Mohammadpourfard, S. Zeinali Heris, Ionic liquids: Promising compounds for sustainable chemical processes and applications, Chem. Eng. Res. Des. 160 (2020) 264–300, https://doi.org/10.1016/j.cherd.2020.06.006.

[16] K. Fukumoto, M. Yoshizawa, H. Ohno, Room temperature ionic liquids from 20 natural amino acids, J. Am. Chem. Soc. 127 (2005) 2398–2399, https://doi.org/10.1021/ja043451i.

[17] C.R. Allen, P.L. Richard, A.J. Ward, L.G.A. van de Water, A.F. Masters, T. Maschmeyer, Facile synthesis of ionic liquids possessing chiral carboxylates, Tetrahedron Lett. 47 (2006) 7367–7370, https://doi.org/10.1016/j.tetlet.2006.08.007.

[18] D.-J. Tao, Z. Cheng, F.-F. Chen, Z.-M. Li, N. Hu, X.-S. Chen, Synthesis and Thermophysical Properties of Biocompatible Cholinium-Based Amino Acid Ionic Liquids, J. Chem. Eng. Data 58 (2013) 1542–1548, https://doi.org/10.1021/je301103d.

[19] A. Costa, A. Forte, K. Zalewska, G. Tiago, Z. Petrovski, L.C. Branco, Novel biocompatible ionic liquids based on gluconate anion, Green Chem. Lett. Rev. 8 (2015) 8–12, https://doi.org/10.1080/17518253.2014.951695.

[20] H. Zhao, DNA stability in ionic liquids and deep eutectic solvents, J. Chem. Technol. Biotechnol. 90 (2015) 19–25, https://doi.org/10.1002/jctb.4511.

[21] R. Vijayaraghavan, A. Izgorodin, V. Ganesh, M. Surianarayanan, D.R. MacFarlane, Long-Term Structural and Chemical Stability of DNA in Hydrated Ionic Liquids, Angew. Chem. Int. Ed. 49 (2010) 1631–1633, https://doi.org/10.1002/anie.200906610.

[22] H. Tateishi-Karimata, N. Sugimoto, Structure, stability and behaviour of nucleic acids in ionic liquids, Nucleic Acids Res. 42 (2014) 8831–8844, https://doi.org/10.1093/nar/gku499.

[23] R.R. Mazid, U. Divisekera, W.J. Yang, V. Ranganathan, D.R. MacFarlane, C. Cortez-Jugo, W.L. Cheng, Biological stability and activity of siRNA in ionic liquids, Chem. Commun. 50 (2014) 13457–13460, https://doi.org/10.1039/c4cc05086j.

[24] C. Mukesh, D. Mondal, M. Sharma, K. Prasad, Rapid dissolution of DNA in a novel bio-based ionic liquid with long-term structural and chemical stability: successful recycling of the ionic liquid for reuse in the process, Chem. Commun. 49 (2013) 6849–6851, https://doi.org/10.1039/c3cc42829j.

[25] M. Sharma, D. Mondal, N. Singh, N. Trivedi, J. Bhatt, K. Prasad, High concentration DNA solubility in bio-ionic liquids with long-lasting chemical and structural stability at room temperature, RSC Adv. 5 (2015) 40546–40551, https://doi.org/10.1039/C5RA03512K.

[26] A. Mishra, M.K. Ekka, S. Maiti, Influence of Ionic Liquids on Thermodynamics of Small Molecule DNA Interaction: The Binding of Ethidium Bromide to Calf Thymus DNA, J. Phys. Chem. B 120 (2016) 2691–2700, https://doi.org/10.1021/acs.jpcb.5b11823.

[27] A. Haque, I. Khan, S.I. Hassan, M.S. Khan, Interaction studies of cholinium-based ionic liquids with calf thymus DNA: Spectrophotometric and computational methods, J. Mol. Liq. 237 (2017) 201–207, https://doi.org/10.1016/j.molliq.2017.04.068.

[28] D.K. Sahoo, S. Jena, J. Dutta, S. Chakrabarty, H.S. Biswal, Critical Assessment of the Interaction between DNA and Choline Amino Acid Ionic Liquids: Evidences of Multimodal Binding and Stability Enhancement, ACS Cent. Sci. 4 (2018) 1642–1651, https://doi.org/10.1021/acscentsci.8b00601.

[29] A.Q. Pedro, P. Pereira, M.J. Quental, A.P. Carvalho, S.M. Santos, J.A. Queiroz, F. Sousa, M.G. Freire, Cholinium-Based Good's Buffers Ionic Liquids as Remarkable Stabilizers and Recyclable Preservation Media for Recombinant Small RNAs, ACS Sustain. Chem. Eng. 6 (2018) 16645–16656, https://doi.org/10.1021/acssuschemeng.8b03900.

[30] G. Gonfa, N. Muhammad, M. Azmi Bustam, Probing the interactions between DNA nucleotides and biocompatible liquids: COSMO-RS and molecular simulation study, Sep. Purif. Technol. 196 (2018) 237–243, https://doi.org/10.1016/j.seppur.2017.08.033.

[31] T.B.V. Dinis, F. Sousa, M.G. Freire, Insights on the DNA Stability in Aqueous Solutions of Ionic Liquids, Front. Bioeng. Biotechnol. 8 (2020), https://doi.org/10.3389/fbioe.2020.547857.

[32] M. v. Quental, A.Q. Pedro, P. Pereira, M. Sharma, J.A. Queiroz, J.A.P. Coutinho, F. Sousa, M.G. Freire,, Integrated Extraction-Preservation Strategies for RNA Using Biobased Ionic Liquids, ACS Sustain. Chem. Eng. 7 (2019) 9439–9448, https://doi.org/10.1021/acssuschemeng.9b00688.

[33] E.V. Capela, A.E. Santiago, A.F.C.S.C.S. Rufino, A.P.M.M. Tavares, M.M. Pereira, A. Mohamadou, M.R. Aires-Barros, J.A.P.P. Coutinho, A.M. Azevedo, M.G. Freire, Sustainable strategies based on glycine–betaine analogue ionic liquids for the recovery of monoclonal antibodies from cell culture supernatants, Green Chem. 21 (2019) 5671–5682, https://doi.org/10.1039/C9GC02733E.

[34] C. Dennison, R. Lovrien, Three phase partitioning: Concentration and purification of proteins, Protein Expr. Purif. 11 (1997) 149–161, https://doi.org/10.1006/prep.1997.0779.

[35] V. Kumar, V. Sathyaselvabala, S.D. Kirupha, A. Murugesan, T. Vidyadevi, S. Sivanesan, Application of Response Surface Methodology to Optimize Three Phase Partitioning for Purification of Laccase from Pleurotus ostreatus, Sep. Sci. Technol. 46 (2011) 1922–1930, https://doi.org/10.1080/01496395.2011.583306.

[36] E. Alvarez-Guerra, A. Irabien, Ionic Liquid-Based Three Phase Partitioning (ILTPP) for Lactoferrin Recovery, Sep. Sci. Technol. 49 (2014) 957–965, https://doi.org/10.1080/01496395.2013.878722.

[37] E. Alvarez-Guerra, S.P.M. Ventura, J.A.P. Coutinho, A. Irabien, Ionic liquid-based three phase partitioning (ILTPP) systems: Ionic liquid recovery and recycling, Fluid Phase Equilib. 371 (2014) 67–74, https://doi.org/10.1016/j.fluid.2014.03.009.

[38] E. Alvarez-Guerra, A. Irabien, Ionic liquid-based three phase partitioning (ILTPP) systems for whey protein recovery: ionic liquid selection, J. Chem. Technol. Biotechnol. 90 (2015) 939–946, https://doi.org/10.1002/jctb.4401.

[39] C.C. Ramalho, C.M.S.S. Neves, M. v. Quental, J.A.P. Coutinho, M.G. Freire,, Separation of immunoglobulin G using aqueous biphasic systems composed of cholinium-based ionic liquids and poly(propylene glycol), J. Chem. Technol. Biotechnol. (2018), https://doi.org/10.1002/jctb.5594.

[40] W. Saenger, Principles of Nucleic Acid Structure, 1st ed., Springer New York, New York, NY, 1984. 10.1007/978-1-4612-5190-3.

[41] M. Petkovic, J.L. Ferguson, H.Q.N. Gunaratne, R. Ferreira, M.C. Leitão, K. R. Seddon, L.P.N. Rebelo, C.S. Pereira, Novel biocompatible cholinium-based ionic liquids—toxicity and biodegradability, Green Chem. 12 (2010) 643, https://doi.org/10.1039/b922247b.

[42] J.F.B. Pereira, K.A. Kurnia, O.A. Cojocaru, G. Gurau, L.P.N. Rebelo, R.D. Rogers, M. G. Freire, J.A.P. Coutinho, Molecular interactions in aqueous biphasic systems composed of polyethylene glycol and crystalline vs. liquid cholinium-based salts, PCCP 16 (2014) 5723–5731, https://doi.org/10.1039/C3CP54907K.

[43] M.V. Quental, M. Caban, M.M. Pereira, P. Stepnowski, J.A.P. Coutinho, M. G. Freire, Enhanced extraction of proteins using cholinium-based ionic liquids as phase-forming components of aqueous biphasic systems, Biotechnol. J. 10 (2015) 1457–1466, https://doi.org/10.1002/biot.201500003.

[44] R. Sadeghi, M. Maali, Toward an understanding of aqueous biphasic formation in polymer–polymer aqueous systems, Polymer (Guildf.) 83 (2016) 1–11, https://doi.org/10.1016/j.polymer.2015.11.032.

[45] R.D.S. Sousa, C. Neves, M.M. Pereira, M.G. Freire, J.A.P. Coutinho, Potential of aqueous two-phase systems for the separation of levodopa from similar biomolecules, J. Chem. Technol. Biotechnol. 93 (2018) 1940–1947, https://doi.org/10.1002/jctb.5553.

[46] A. Luís, T.B.V. Dinis, H. Passos, M. Taha, M.G. Freire, Good's buffers as novel phase-forming components of ionic-liquid-based aqueous biphasic systems, Biochem. Eng. J. 101 (2015) 142–149, https://doi.org/10.1016/j.bej.2015.05.008.

[47] G.T. Dee, T. Ougizawa, D.J. Walsh, The pressure-volume-temperature properties of polyethylene, poly(dimethyl siloxane), poly(ethylene glycol) and poly(propylene glycol) as a function of molecular weight, Polymer (Guildf). 33 (1992) 3462–3469, https://doi.org/10.1016/0032-3861(92)91104-A.

[48] M.C.M. Sequeira, M.F.V. Pereira, H.M.N.T. Avelino, F.J.P. Caetano, J.M.N. A. Fareleira, Viscosity measurements of poly(ethyleneglycol) 400 [PEG 400] at temperatures from 293 K to 348 K and at pressures up to 50 MPa using the vibrating wire technique, Fluid Phase Equilib. 496 (2019) 7–16, https://doi.org/10.1016/j.fluid.2019.05.012.

[49] I.A. Shkel, D.B. Knowles, M.T. Record, Separating chemical and excluded volume interactions of polyethylene glycols with native proteins: Comparison with PEG effects on DNA helix formation, Biopolymers 103 (2015) 517–527, https://doi.org/10.1002/bip.22662.

[50] J.A. Sikorsky, D.A. Primerano, T.W. Fenger, J. Denvir, Effect of DNA damage on PCR amplification efficiency with the relative threshold cycle method, Biochem. Biophys. Res. Commun. 323 (2004) 823–830, https://doi.org/10.1016/j.bbrc.2004.08.168.

[51] R. Mazid, M.X. Tan, M.K. Danquah, Molecular Delivery of Plasmids for Genetic Vaccination, Curr. Pharm. Biotechnol. 14 (2013) 615–622, https://doi.org/10.2174/138920101131400226.

[52] I. Zupanič Pajnič, G. Marrubini, B.G. Pogorelc, T. Zupanc, C. Previderè, P. Fattorini, On the long term storage of forensic DNA in water, Forensic Sci. Int. 305 (2019) 110031, https://doi.org/10.1016/j.forsciint.2019.110031.

[53] K.D. Clark, M. Sorensen, O. Nacham, J.L. Anderson, Preservation of DNA in nuclease-rich samples using magnetic ionic liquids, RSC Adv. 6 (2016) 39846–39851, https://doi.org/10.1039/c6ra05932e.

[54] J.G. Baust, Strategies for the Storage of DNA, Biopreserv Biobank. 6 (2008) 251–252, https://doi.org/10.1089/bio.2008.0604.lett.

[55] M. Vorlíčková, I. Kejnovská, K. Bednářová, D. Renčiuk, J. Kypr, Circular Dichroism Spectroscopy of DNA: From Duplexes to Quadruplexes, Chirality 24 (2012) 691–698, https://doi.org/10.1002/chir.22064.

[56] QIAGEN, QIAGEN Plasmid Kits, https://www.qiagen.com/us/products/discovery-and-translational-research/dna-rna-purification/dna-purification/plasmid-dna/qiagen-plasmid-kits?fbclid=IwAR2LNUaFsliDYF0a3IxMCPP74o4DjOnI087VW0KeWy96iIqX_OYZfh4Tss&catno=12143, 2023 (accessed 12 March 2023).

[57] MERCK, Choline bicarbonate, https://www.sigmaaldrich.com/PT/en/product/sigma/c7519, 2023 (accessed 12 March 2023).

[58] MERCK, Glycolic acid, https://www.sigmaaldrich.com/PT/en/substance/glycolicacid760579141, 2023 (accessed 12 March 2023).

[59] MERCK, Poly(ethylene glycol), https://www.sigmaaldrich.com/PT/en/product/aldrich/202398?&msclkid=6d73bdb95f181021d09bd9b7477559c2&utm_source=bing&utm_medium=cpc&utm_campaign=LSC_aldrich_misc_NA_(bing%20ebizpfs)&utm_term=peg400&utm_content=aldrich%2F202398&gclid=6d73bdb95f181021d09bd9b7477559c2&gclsrc=3p.ds, 2023 (accessed 12 March 2023).